NUMERICAL SIMULATION OF TRANSONIC SHOCK-VORTEX INTERACTION FLOW AROUND THE VFE-2 DELTA WING BASED ON MDDES

Zhao Ke, Gao Zheng-hong, Huang Jiang-tao
National key laboratory of aerodynamic design and research, School of Aeronautics, Northwestern Polytechnical University, Xi'an city, P.R.China
zhaowangshui@163.com;zgao@nwpu.edu.cn

Keywords: *shock/vortex interactions, MDDES, cross-flow shock, vortex breakdown*

Abstract

The transonic flow around the 65° Delta wing configuration with sharp leading edge is presented. The occurrence of shock on delta wings introduces complex shock/vortex interactions, particularly at moderate-to-high angles of incidence. These interactions can make a significant difference to the vortex breakdown. Transonic vortical flow and vortex breakdown is one aspect of the second "International Vortex Flow Experiment" (VFE-2). This investigation considers complex flowfield the 65° Delta wing using modified delayed detached eddy simulation(MDDES).

The time-averaged pressure is compared with the experiment data to validate the method. The shocks in the flow field are investigated and the interaction of the vortex and the shock waves is also studied. The unsteady characteristic of the vortex breakdown is analyzed by studying the Power Spectral Density (PSD) of time history of density at the probe points.

1 Introduction

The modern fighters request subsonic and transonic maneuverability as well as supersonic cruise characteristics, so vortex configurations are widely used in modern fighter. And the breakdown of vortex is very important for the aerodynamic characteristics and the safety of the aircraft, the vertical flow around delta wing is typical vortex configuration, so it is studied mostly. The subsonic behavior of the flow and vortex breakdown is fairly well understood. The behavior of the delta wing vortical flow under transonic conditions is not well understood. Within this regime, complex interactions between shockwaves and the leading edge vortex system occur at moderate to high angle of attack. For this reason, transonic vortical flow and vortex breakdown is one aspect of the second "International Vortex Flow Experiment" (VFE-2) [1, 2]. The occurrence shockwave systems [3] in the flow introduce the complex behavior of shock/vortex interactions (Figure1). These interactions have a significant effect on vortex breakdown and the breakdown behavior is quite different to subsonic vortical flows where the onset of breakdown is relatively gradual with increasing incidence. The onset of transonic breakdown is a sudden and

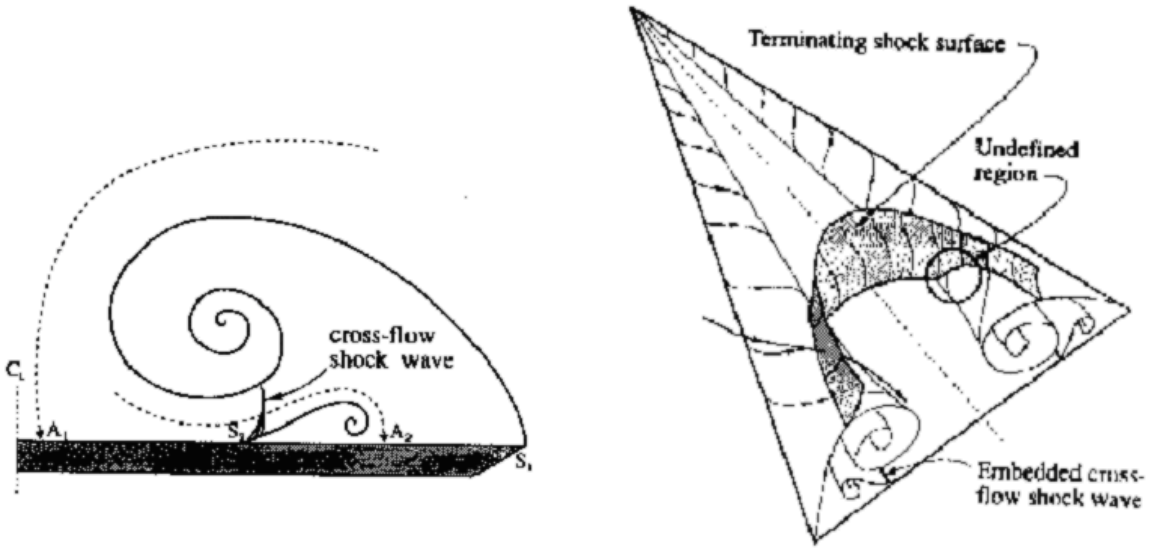

(a) Embedded cross-flow shock wave (b) Rear/terminating shock surfaces

Fig.1. Schematic Diagrams Showing Proposed Positionsand Phapes of Shock Systems over Transonic Delta Wing

complete loss of suction on the wing characterized by the collapse of the surface pressure distribution suction peak. The pressure distributions downstream of breakdown are quite flat. This has obvious bad effects on the aerodynamic performance of the wing, particularly when coupled to the abrupt nature of the breakdown. Aerodynamic characteristics such as lift coefficient distribution stall and pitch may all be badly affected by such flow behavior. The shock/vortex interactions and vortex breakdown are essentially unsteady process, the traditional Reynolds averaged Navier-Stokes (RANS) method fail to accurately predict flow structures in separated-flow regions and small vortex structure because they resolve only a portion of the turbulence scales of interest. Delayed Eddy Simulation (DES) use RANS in the near-wall region and (Large Eddy Simulation) LES in the separated region leads to a basic question about the accuracy of the resulting solution notably in turbulence parameters being computed. So MDDES [4] method is used in this paper to investigation the transonic flow around VFE-2 delta wing.

2 65° VFE-2 Delta Wing and Grid Generation

The geometry used for this calculations is the 2nd International Flow Experiment (VFE-2) proposed by Hummel and Redecker. The geometry is originally used in experiments carried out by Chu and Luckring in the National Transonic Facility (NTF) at NASA Langley. These experiments considered a 65° delta wing with four leading edge profiles (one sharp and three rounded with small, medium and large radii) for a wide range of conditions both subsonic and transonic and for both test and flight Reynolds numbers. This data has been compiled into a comprehensive experimental database and forms the basis for the investigations of the VFE-2. The geometry is analytically defined for all leading edge profiles, which allows improved correlation between experimental and computational results by reducing geometrical discrepancies. For this investigation, only

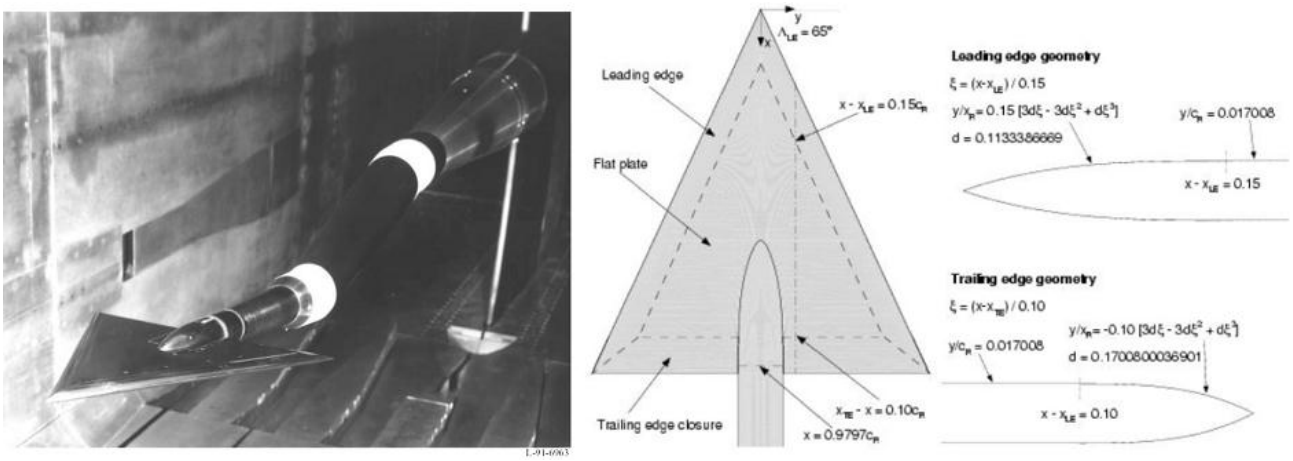

Figure 2 Wing geometry used in investigation

the sharp leading edge profile is considered. Figure 2 shows the wing situated in the NTF wind tunnel and a brief overview of the analytical dimensions of the wing. All calculations were performed at a Mach number of M = 0.85 and Reynolds number, based on the mean aerodynamic chord, of Re = 6 × 10^6 and for an incidence of α= 18.5 ° and α= 23 °.

The structured multi-block grid was created firstly. The semi-span geometry was reproduced to approximately one chord length downstream of the trailing edge, at which point an approximation to the experimental sting (See Figure 2) was made to the far field. This accuracy of the sting was chosen because the effect of a sting or support apparatus was negligible downstream of a distance one root chord from the trailing edge. An H-H topology was chosen for the wing with a collapsed edge, a structured O-grid was used around the sting. Overall, the blocking structure was optimized for cell geometry and therefore, reduced skewness, particularly in the sting tip region and as a result a total of 400 blocks were used. The overall size of the grid was approximately 1.3×10^7 grid points. The first wall spacing used was 1 × 10^{-5}cr, and there are approximately 29 grid points in the boundary layer region (Figure 3).

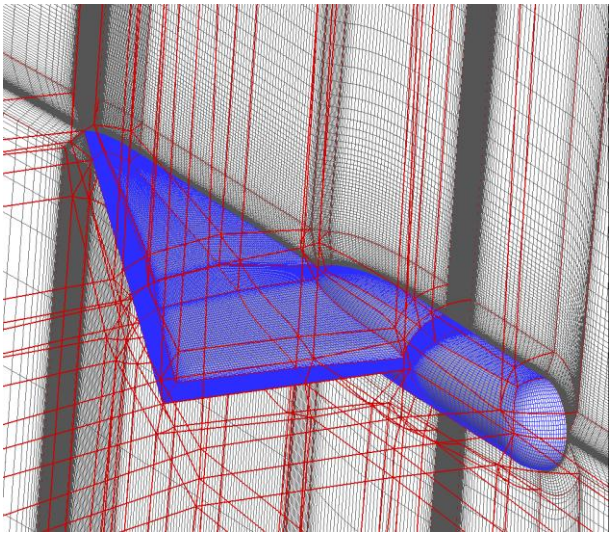

Figure 3 the computational grid for this paper

3 Computational Methods

3.1 Flow Solver

The basic program in this paper is a structured, finite-volume, compressible, Reynolds-averaged Navier-Stokes solver developed in our research group. The Roe flux-difference scheme is used for calculating inviscid fluxes and a second-order central scheme is used to discretize the viscous terms. The second-order upwind scheme is used for calculating convection term of turbulent

model equation and transition model equations. The implicit approximate-factorization method is used for time advancing. The farfield boundary conditions are implemented using the 1-D characteristic-based Riemann invariants to avoid spurious wave reflections at the computational domain boundaries. The no-slip viscous surface boundary is used at the wall. Two pieces of auxiliary information are supplied with normal pressure gradient $\partial p/\partial n = 0$ and adiabatic wall condition $\partial T/\partial n = 0$. Where n is outer normal direction of the wall.

3.2 Turbulence Models

Menter's $k-\omega$ SST [5] equations are:

$$\rho\frac{\partial k}{\partial t}+\rho u_j\frac{\partial k}{\partial x_j}=P_k-\beta^*\rho k\omega+\frac{\partial}{\partial x_j}[(\mu+\mu_t/\sigma_k)\frac{\partial k}{\partial x_j}] \quad (1)$$

$$\rho\frac{\partial \omega}{\partial t}+\rho u_j\frac{\partial \omega}{\partial x_j}=P_\omega+\frac{\partial}{\partial x_j}[(\mu+\mu_t/\sigma_\omega)\frac{\partial \omega}{\partial x_j}]-\beta\rho\omega^2+2(1-F_1)\sigma_{\omega 2}\frac{1}{\omega}\frac{\partial k}{\partial x_j}\frac{\partial \omega}{\partial x_j} \quad (2)$$

where the source is defined as:

$$P_k=\mu_t S_{ij}S_{ij} \quad (3)$$

and S_{ij} is strain tensor.

the eddy viscosity is :

$$\mu_t=\min(\frac{\rho k}{\omega},\frac{a_1\rho k}{\Omega F_2}) \quad (4)$$

3.3 Modified Delayed Detached Eddy Simulation

DES method is a hybrid RANS/LES method introduced by Spalart[6], first coupled with S-A turbulence model. The DES version of the SST derived by Strelets [7] replaces the dissipation term in the turbulent kinetic energy equation ($\beta^*\rho k\omega$) with:

$$\rho k^{3/2}/l_{k-w} \quad (5)$$

Where $l_{k-w}=\min(\beta^*\sqrt{k}/\omega, C_{des}\Delta)$, Δ is a grid length scale defined by:

$$\Delta=max(\Delta x,\Delta y,\Delta z) \quad (6)$$

And Δx , Δy , Δz is local grid lengths.

Although the DES model has been often used for solving unsteady separated flows, this model depends too strongly on the grid quality and topology, and can lead to non-physical results with grid refinement in viscous layers. Spalart [8] have recently modified the DES model to overcome some of the shortcomings related to its grid dependence in a new model named Delayed Detached Eddy Simulation (DDES). The DDES model applies a blending function based on f_d to the destruction terms in the turbulence equation. The function f_d varies between 0 for RANS mode and 1 for LES mode. In this paper the method is extended to SST-DES model:

$$f_d=1-tanh\left([8r_d]^3\right) \quad (7)$$

where $r_d=\frac{v_t+v}{\sqrt{U_{i,j}U_{i,j}}\kappa^2 d^2}$, $U_{i,j}=\frac{\partial U_i}{\partial x_j}$ is the (i , j)'th component of stress tensor, and d is the distance from the field point to the nearest wall, κ is Karman const ,the value is 0.41.

Then f_d is applied to the model by

the equation:

$$l_{k-w} = \beta^* \sqrt{k} / \omega - f_d max(0, \beta^* \sqrt{k} / \omega - C_{des}\Delta) \quad (8)$$

A pocket of large eddy-viscosity is detected in regions upstream of the cylinders in initial application of the DDES model. In order to overcome such non-physical behavior, the blending function is also applied to the production terms. However, to retain the same near wall behavior, the function is only applied to the production terms when $f_d > C_{MDD}$. The new blending function has the form

$$f_m = \frac{1 - f_d}{1 - C_{MDD}} \quad (9)$$

In this paper C_{MDD} is 0.975 given by Veer N. Vatsa [4]. The modified turbulence model can be written in dimensional form as:

$$\rho \frac{\partial k}{\partial t} + \rho u_j \frac{\partial k}{\partial x_j} = f_m P_k - \rho k^{3/2} / l_{k-w} + \frac{\partial}{\partial x_j}[(\mu + \mu_t / \sigma_k) \frac{\partial k}{\partial x_j}] \quad (10)$$

4 Result and Discussion

4.1 Numerical Result and Experiment Data

Computational time averaged pressure coefficient is compared with the experimental pressure coefficient distributions at five streamwise locations on the wing surface, x/cr = 0.2, 0.4, 0.6, 0.8 and 0.95. The results of these validation comparisons are shown in Figure 4 for both incidences, with the computational results being compared to the corresponding experimental data points. A sensitivity study of the flow to a number of computational factors, such as turbulence model, is also undertaken by comparing MDDES results to RANS results of SA and SST turbulence model. And it is found that MDDES have great effect on the overall behavior of the transonic vortical flow due to accurately grasping the unsteady characteristics of the flow field. Time-dependent flowfield is analyzed to explain the post breakdown development of the main vortical structures and also the complex interaction between vortex breakdown and the shock system ahead of the sting. It is shown that the result predicted by MDDES is much better agree with the experimental data than the RANS. For most streamwise locations, the magnitudes and positions of the suction peaks are well predicted; the secondary vortex is under-predicted in the solution. This may be improved by grid refinement and transition model. It is also shown that after the shock the result becomes worse because of the complex shock/vortex interactions, which may be improve by increase the grid as well as the integral time steps. It is clear that the peak value of pressure coefficient becomes week due to the break down of primary vortex.,the lift will lost greatly as indicate by Houtman E M. Bannink B J [9].

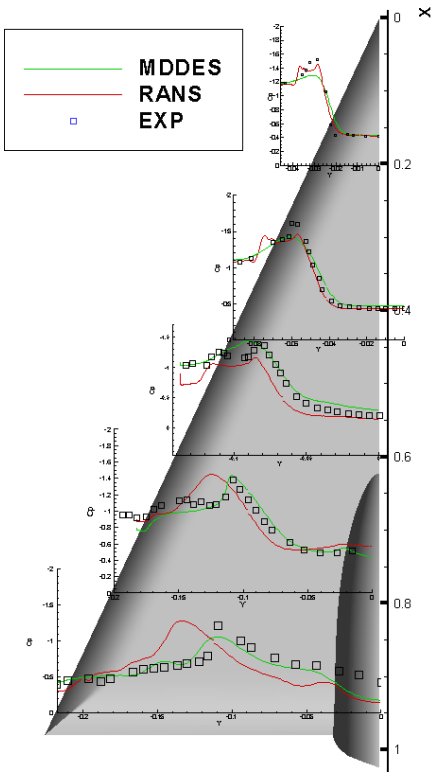

(a) Pre-breakdown Case,α= 18.5°

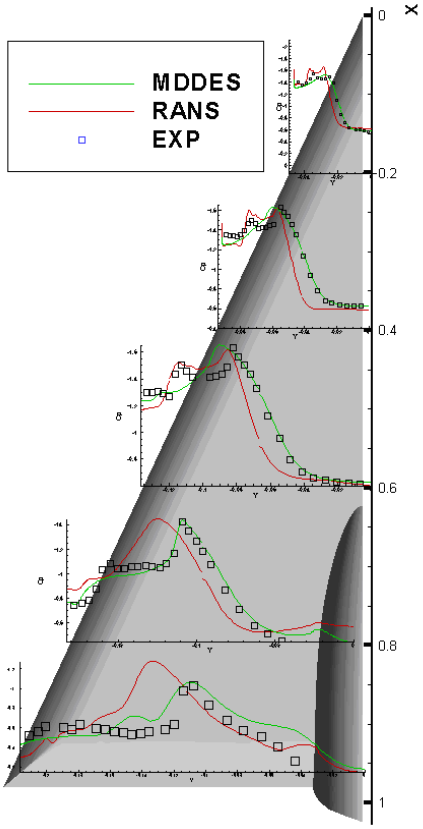

(b) Post-breakdown Case, α= 23 °

Figure 4 Comparisons between Computational Results and Experiment for M = 0.85, Re = 6×10^6

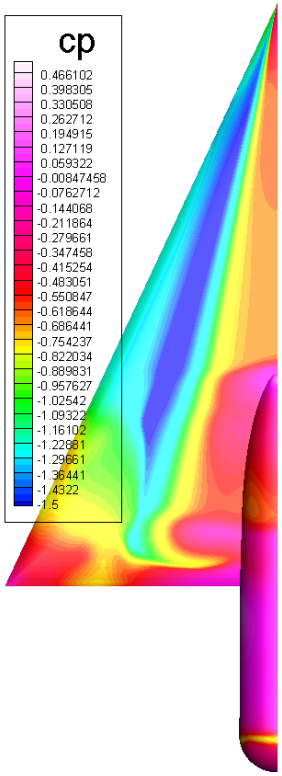

(a) Pre-breakdown Case,α= 18.5°

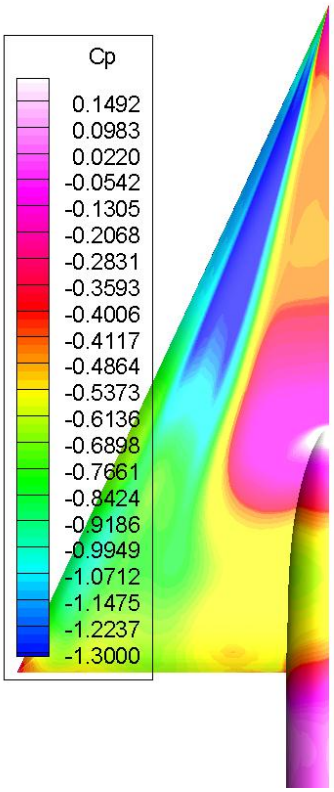

(b) Post-breakdown Case, α= 23°

Figure 5 Surface Pressure Coefficient Contours for the Wing for M = 0.85, Re = 6×10^6

The surface pressure coefficient

contours of two incidences are shown in (Figure5).it is shown that the shock position of α= 23° case is more and strong than the low incidence case by comparing the contour, and the vortex breakup earlier than the α= 18.5 ° case due to the shock wave in the flow field. The breakdown of the vortex of α = 23 ° case is caused by the shock beside the sting.

4.2 Shocks in The Flow

Normal shocks [10, 11] occurring in the flow are determined by plotting the pressure coefficient along the symmetry plane as shown in Figure 6. It is shown that there are two normal shocks occurring at the symmetry plane. For an incidence of 18.5 ° ,the first occurs upstream of the sting tip at approximately x/cr = 0.6, caused by the sting geometry. Further downstream at approximately x/cr = 0.9 a second shock is found. The second shock is likely to correspond to the rear/terminating shock. A third compression region is also found close to the trailing edge, and a third shock is found from the surface pressure contours at this location outboard of the symmetry plane on the wing surface. A shock occurring at this location is likely to be caused by the high curvature of the wing geometry and the necessity of the flow to return to freestream conditions at the trailing edge. For an incidence of 23 ° , the behavior at the symmetry plane shows the shock at the sting tip at approximately x/cr = 0.6, but with a second shock occurring in the flow slightly upstream of this location, at approximately x/cr = 0.5, and the strength of the shock at the sting is much stronger than the 23 ° case. So the vertex is breaking down when passing this shock. It is clear that the rear/ terminating shock described for the 23 ° case is no longer evident and that a new second shock is apparent upstream of the sting tip.

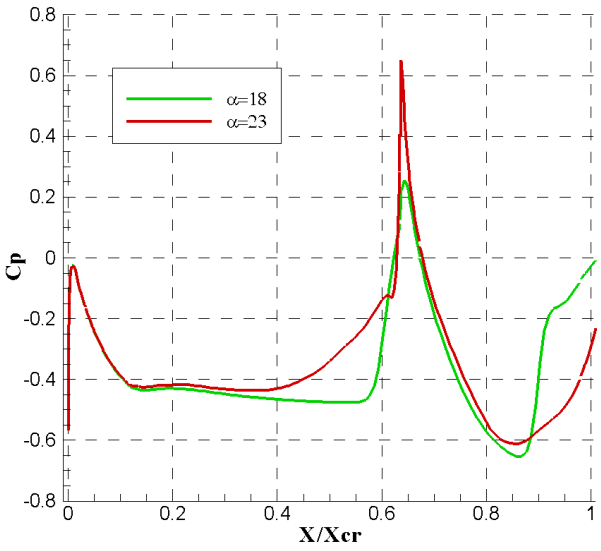

Figure 6 Pressure Coefficient Distributions at The Symmetry Plane on The Wing

Three-dimensional behavior of the normal shocks, it is found that the shock occurring upstream of the sting tip curves downstream and intersects the rolled up shear layer of the vortex as shown in Figure 7 highlighted by the dashed lines. This is consistent with the schematic shown in Figure 1 for the rear/terminating shock. However, it is likely that this curvature is caused by the sting presence for this configuration. Also highlighted are the locations of the other normal shocks found in the flow and described above, the position and form of the shock is quite consistent with the result of L. A. Schiavetta [12]. The rear/terminating shock in the 18.5 ° solution is found to be normal to the freestream and wing surface and does not appear to curve downstream outboard of the symmetry plane. This lack of curvature may due to the influence of the sting on the flow, as the

previous investigations have considered a flat wing

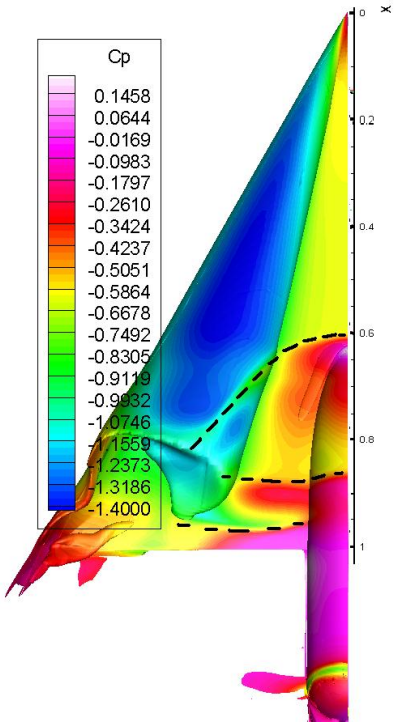

(a) Pre-breakdown Case,α= 18.5°

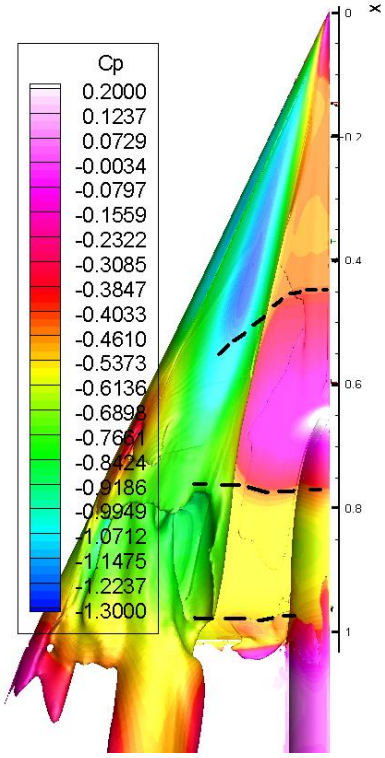

(b) Post-breakdown Case, α= 23°

Fig.7. Isosurface of x Vorticity Coloured by Pressure Coefficient Showing Primary Vortex Shear Layer and Normal Shock Shape

without sting support. Also clear from this plot are the two cross-flow shocks which sit above the vortex. It is possible, for both incidences, that there is an interaction between these cross-flow shocks and the normal sting tip shock, which will further increase the complexity of the flow in this region. However, further experimental data is needed in this region to determine this behavior.

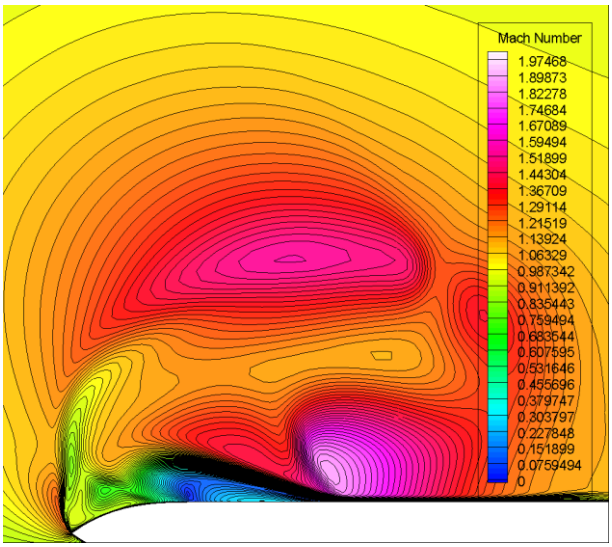

(a) α =18.5 °(x/cr=0.8)

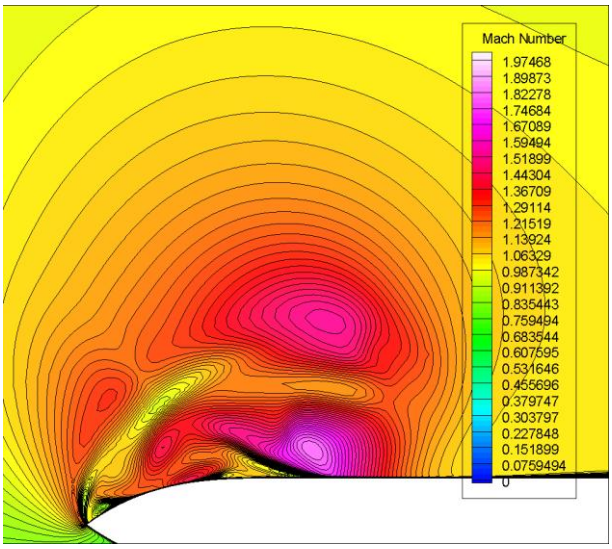

(b) α = 23 °(x/cr=0.4)

Fig.8 Contours of Mach Number Showing the Cross Flow Shock

The flow structure in a plane normal to the wing surface and the freestream direction is investigated to show a

complex cross-flow shock system, beneath and around the primary and secondary vortices. Figure 8 shows the Mach contours at x/cr = 0.8 for α = 18.5 ℃ase and at x/cr = 0.4 for α = 18.5 °.The cross-flow shocks beneath and around the primary and secondary vortices are shown on the contour plots. These sharp changes in Mach number indicate the presence of cross-flow shocks as described in the introduction and shown in Figure 1, both these shocks are likely to be caused by the curvature of the shear layer causing the flow to accelerate up to conditions which cannot be sustained.

4.3 Shock/Vortex Interaction and Vortex Breakdown

It appears that the sting tip shock intersects the vortex system and therefore it is highly likely that some form of shock/vortex interaction takes place, particularly for higher incidences. An instantaneous shock and streamline around the delta wing is shown in figure9, and the shock is shown by iso-surface of pressure gradient in the space. It is clear from figure 9 that the norm shock waves before the sting intensively interact with the primary vortices and due to the large pressure gradient across the shock, the vortex is breakdown. To further consider this, the pressure in the free stream direction through the vortex cores for both incidences is analyzed in Figure10. For the 18.5 ° case, the interactions occur without vortex breakdown, and this is due to the shock sitting above the vortex core.However, from consideration of the vortex core properties it is found that there are two regions of adverse pressure gradient which may suggest direct interactions. The first interaction is weak, and the primary vortex recovers after passing through each. The second is a strong pressure gradient at the trailing edge and the vortex is breakdown. For the 23 ° case, the breakdown occurs on the wing, it is clear high adverse pressure gradient at the vortex core coinciding with the location of the normal shock upstream of the sting tip and with the onset of vortex breakdown. From analysis of the solutions, it is determined that the onset of vortex breakdown is highly dependent on the vortex strength and the strength and location of the shocks in the flow. Figure 11 shows a contour of Q on a x/cr = 0.85 plane, it can be seen that after breakdown , the centralized vortex break to pieces of small vortex structural, and the MDDES can give a more fine flow feature.

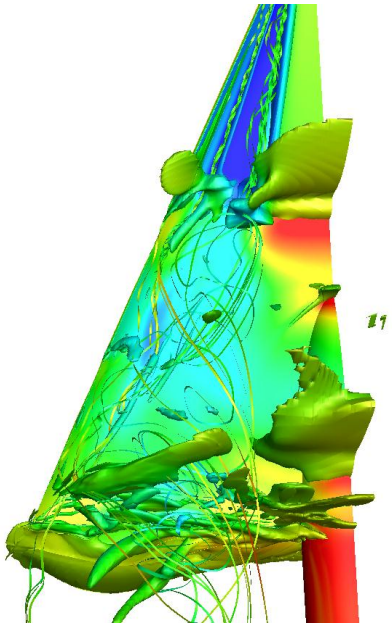

Fig.9 Shock Contour and Streamline around the Delta Wing

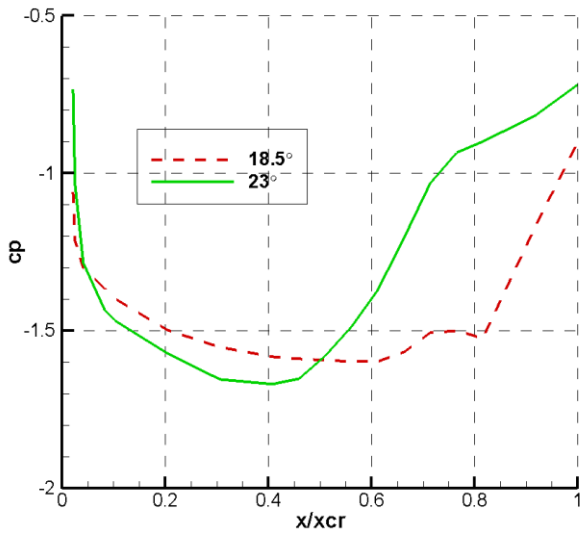

Fig.10. Pressure Coefficient Distributions through Vortex Cores

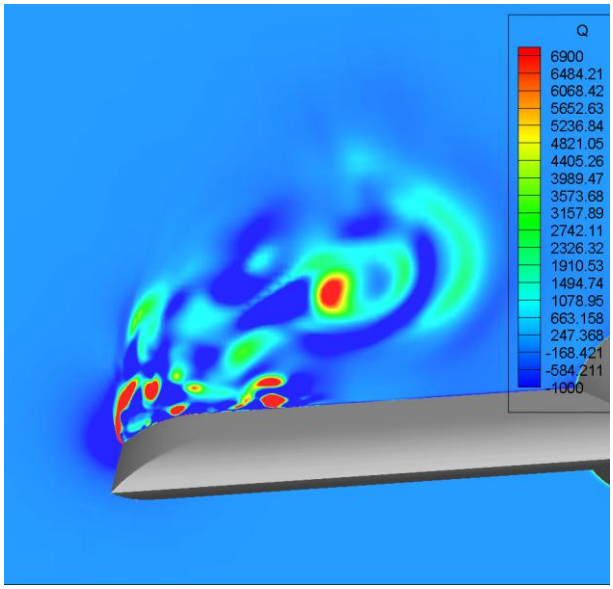

Figure 11 Contour of Q on a x/cr = 0.85 Plane

Since the shock-vortical interaction and vertical breakdown is an unsteady process [13,14], and MDDES method computes a time accuse flow, the variety of flow variable can be recorded to analyze the unsteady characteristics of the flow around the delta wing. Six probe points is chose to track the variable of density at these points to analyze the flow feature, shown in figure 12. Figure 13 shows the time history of the fluctuating density. The FFT is done to the data at different point, and figure 14 shows the PSD of density if the probe points. It is clear that there are three peak value of the PSD, corresponding to the three vortexes in the flow field, the highest is the primary vertical, and the abscissa shows the frequency of the vortex breakdown oscillation frequencies. Also the other two points correspond to the other vortex breakdown oscillation frequencies. It is also can be seen that the value of PSD is variety at the different points. The max value is probe 4 locating just after the break point of the vortex and at the region below the vortex. Probe 6 locate at the region that the other two vertical breakdown, corresponding to the max value of other two vortex. The probe 3 and 5 locate away from the vortex, so the vortex oscillation slightly affects it, and the max value is not that evident.

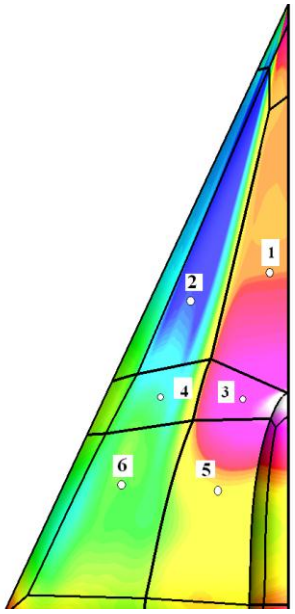

Fig.12. The Distribution of Probe Points on The Wing

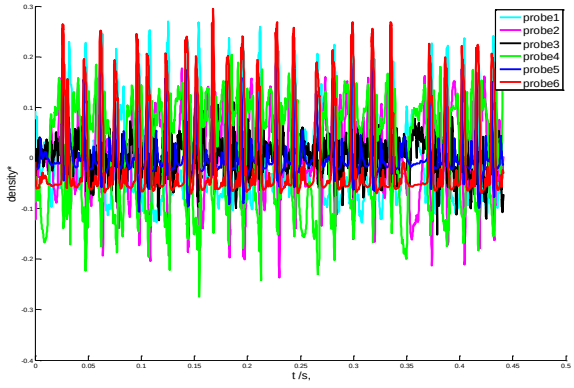

Fig.13. Time History of Fluctuating Density

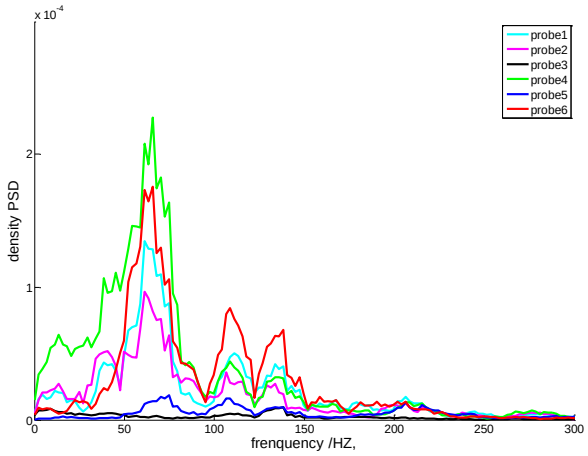

Fig.14. Power Spectral Density Plots of Unsteady Density of Probe Data

5 Conclusions

The transonic flow around VEF-2 delta wing is investigated in this paper, the vortex/shock interaction and vortex breakdown is analyzed by MDDES. The time-averaged pressure coefficient and pressure contour are compared with the experiment data to validate the method in this paper. It is shown that the MDDES method can well simulate the complex flow feature around the delta wing.

The shock waves in flow field are investigated, it is shows that the shock waves are very complex because they are not only induced by the sting of the model, the shock waves also exists between the vortex cores, which induces a very large velocity field upon the wing, the velocity is so large that the shockwaves are induced and interacting with the vortex.

The breakdown of vortex is very complex especially in the transonic flow, the shock waves will interact with the vortex and can suddenly make it breakdown which is much more different form the subsonic cases. The unsteady chiastic of the vortex breakdown induced by the shock waves in the flow is analyzed by the PSD method.

Copyright Statement

Reference:

[1] Elsenaar, A. and Hoeijmakers, H. W. M. An experimental study of the flow over a sharp-edged delta wing at subsonic and transonic speeds. *AGARD Conference Proceedings "Vortex Flow Aerodynamics"*, AGARD-CP-494, July 1991, pp. 15.1–15.19

[2] Chu, J. and Luckring, J.M. Experimental surface pressure data obtained on a 65° delta wing across Reynolds number and Mach number ranges: Volume1-Sharp Leading Edge. *NASA Technical Memorandum*

4645,NASA Langley Research Centre, Feb.1996.

[3] Donohoe, S.R. and Bannink,W.J. Surface reflective visualisations of shock-wave /vortex interactions above a delta wing. *AIAA Journal*, Vol.35, No.10, 1997, pp.1568-1573

[4] Veer N. Vatsa,DavidP.Lockard. Assessment of Hybrid RANS/LES turbulence model for aeroacoustics applications. *6th AIAA/CEAS Aeroacoustics Conference*.AIAA-2010-401.

[5] Menter, F. R. Two-equation eddy-viscosity turbulence models for engineering applications. *AIAA Journal*, Vol. 32, No. 8, 1994, pp. 1598–1605.

[6] Spalart, P.R., Jou, W.-H., Strelets, M., Allmaras, S.R. Comments on the feasibility of LES for wngs, and on a Hybrid RANS/LES approach, advances in DNS/LES. *1st AFOSR Int. Conf. on DNS/LES*, Greyden Press, Columbus Oh., 1997.

[7] Strelets, M. Detached Eddy Simulation of Massively Separated Flows.*39th AIAA Aerospace Sciences Meeting and Exhibit*, AIAA paper2001-0879, Jan. 2001.

[8] Spalart, P. R., Deck, S., Shur, M. L., Squires, K. D., Strelets, M. Kh., and Travin, A. A new version of Detached-Eddy Simulation, resistant to ambiguous grid densities. *Theoretical Computational Fluid Dynamics*, Vol. 20, 2006, pp. 181-195.

[9] Houtman E M. Bannink B J.Experimental and numerical investigation of the vortex flow over a delta wing at transonic speeds[A] . *AGARD Conference Proceedings Vortex Flow Aerodynamics* , AGARD-CP-494 , July 1991：5.1-5.11

[10] Longo, J. M. A.Compressible inviscid vortex flow of a sharp edge delta wing.*AIAA Journal*, Vol. 33, No. 4, 1995, pp. 680-687.

[11] Donohoe, S. R., Houtman, E. M., and Bannink, W. J. Surface reflective visualization system study to vortical flow over delta wings.*Journal of Aircraft*, Vol. 32, No. 6, 1995, pp. 1359–1366.

[12] L. A. Schiavetta, O. J. Boelens, S. Crippa, R. M. Cummings, W. Fritz ,K. J. Badcock. Shock effects on delta wing vortex breakdown. *Journal of Aircraft*, Vol. 46, No. 3, May–June 2009.

[13] Andrej Furman, Christian Breitsamter. Turbulent and unsteady flow characteristics of delta wing vortex systems vortical flows over delta wings. *46th AIAA Aerospace Sciences Meeting and Exhibit*, AIAA paper 2008-381, January 2008.

[14] Russell M. Cummings, Andreas Schutte. Detached-Eddy Simulation of thevortical flowfield about the VFE-2 delta wing. *46th AIAA Aerospace Sciences Meeting and Exhibit*, AIAA paper 2008-396, January 2008